A Two-Level Sensorless MPPT Strategy Using SRF-PLL on a PMSG Wind Energy Conversion System

Amina ECHCHAACHOUAI[1], *Soumia EL HANI*[1], *Ahmed HAMMOUCH*[2], *Imad ABOUDRAR*[1]

[1]Department of Electrical Engineering, Ecole Normale Superieure de Enseignement Technique, Mohammed V University, Avenue des Nations Unies, Agdal, 10102 Rabat, Morocco
[2]National Center for Scientific and Technical Research, Angle avenues des FAR et Allal El Fassi, Hay Ryad, 10102 Rabat, Morocco

amina.echchaachouai@um5s.net.ma, s.elhani@um5s.net.ma, hammouch_a@yahoo.com, imad.aboudrar@um5s.net.ma

DOI: 10.15598/aeee.v15i3.2193

Abstract. *In this paper, a two-level sensorless Maximum Power Point Tracking (MPPT) strategy is presented for a variable speed Wind Energy Conversion System (WECS). The proposed system is composed of a wind turbine, a direct-drive Permanent Magnet Synchronous Generator (PMSG) and a three phase controlled rectifier connected to a DC load. The realised generator output power maximization analysis justifies the use of the Field Oriented Control (FOC) giving the six Pulse Width Modulation (PWM) signals to the active rectifier. The generator rotor speed and position required by the FOC and the sensorless MPPT are estimated using a Synchronous Reference Frame Phase Locked Loop (SRF-PLL). The MPPT strategy used consists of two levels, the first level is a power regulation loop and the second level is an extremum seeking bloc generating the coefficient gathering the turbine characteristics. Experimental results validated on a hardware test setup using a DSP digital board (dSPACE 1104) are presented. Figures illustrating the estimated speed and angle confirm that the SRF-PLL is able to give an estimated speed and angle which closely follow the real ones. Also, the power at the DC load and the power at the generator output indicate that the MPPT gives optimum extracted power. Finally, other results show the effectiveness of the adopted approach in real time applications.*

Keywords

Direct-drive PMSG, extremum seeking, FOC, sensorless two-level MPPT, SRF-PLL, WECS.

1. Introduction

The Earth receives every day an infinite renewable energy that we can exploit to increase sustainable development. The extracted energy is integrated in the ecosystem that stimulates the growth of new expertise, creates jobs and ensures the energy future. Among all known forms of renewable energy, wind energy conversion has become a major producer of electric power [1].

Recent research in this field is focused on minimizing the overall cost of the Wind Energy Conversion System (WECS) while improving the quality of the produced power. In order to achieve this objective, several works have been carried out to avoid the use of the mechanical sensors which are expensive to buy and maintain. These sensors are usually implemented to measure the generator rotation speed as well as the angle of the rotor that are necessary for the general control of the system and the search for the maximum points of the extractable power.

With the same principle, we consider for investigation in this work a WECS consisting of a wind turbine, a direct-drive Permanent Magnet Synchronous Generator (PMSG), a three phase active rectifier connected to a DC load. The PMSG choice is very advantageous [2], it allows direct-drive systems that avoid gearbox [3] use and this leads to low maintenance constraints. This type of machines is characterized by a high-power density and high efficiency (as there are no copper losses). The use of permanent magnets for the excitation consumes no extra electrical power. The absence

of mechanical commutator and brushes or slip rings implies low mechanical friction losses. Finally, the PMSG drives achieve very high torque at low speeds with less noise.

Based on a generator output power maximization analysis, the Field Oriented Control (FOC) is implemented [4] to control the active rectifier whose performance compared to a diode rectifier has been confirmed in a previous work [6].

Betz limit [5] indicates that the maximum power that can be extracted from the wind is limited to approximately 0.59 of the kinetic energy. The power coefficient C_p, included in the expression of the generated power, takes into consideration this limit and varies with the rotational speed of the turbine. In a different way, the maximum points of the power vary with the wind speed and this justifies the implementation of a Maximum Power Point Tracking (MPPT) strategy to keep our system available to generate optimal power and improve its performance.

To reduce the cost of a WECS, a profitable solution is the sensorless MPPT that allows avoiding the use of mechanical sensors and then improving the relative cost/quality of the complete system. For this reason, there are many estimators used to estimate the generator rotor speed and position required by the FOC and the MPPT. In our previous works, two types of estimators were implemented; The fisrt is the Angle Tracking Observer (ATO) [6] and the second is the Extended Kalman Filter (EKF) [7]. In this work, we adopt a mechanical sensorless MPPT strategy that uses a Synchronous Reference Frame Phase Locked Loop (SRF-PLL) as estimator. It should be noted that the advantage of the SFR-PLL is that it avoids the double-frequency error problem of single-phase standard PLL. It has a simple structure that offers ease of parameter tuning and robust features.

The MPPT strategy adopted is a two-level strategy. The first level is the power regulation loop that gives the reference value of current iq_{ref} to the FOC. A method of extremum seeking [8] is involved as a second level of the MPPT algorithm to generate the optimum value of the coefficient including turbine parameters in the expression of the output power. This coefficient is needed in the first level. Estimating this coefficient allows realizing this approach even when the turbine parameters are not determined.

This work is organized as follows: The first part presents the system modeling by detailing the equation models of both the different components of the wind conversion system considered and the control applied to the active rectifier and by giving their detailed structure illustrated in Fig. 1. The second part concerns the sensorless two-level MPPT strategy adopted and explains the estimators used. The third part gives the results obtained on the experimental test bed setup that enables the evaluation of the approach discussed in this paper.

2. System Modeling

Figure 1 presents the system considered in this work for investigation. It consists of two main parts; the hardware setup gathering elements of the wind energy conversion system which are: a wind turbine, a direct-drive PMSG connected to a three phase rectifier supplying a DC load, and the analog board dSPACE 1104 containing analog to digital and digital to analog converters making connection between the Real-Time Interface (RTI) in the monitoring PC and the hardware possible. In the interface, the Simulink model of the global control is implemented giving-out six Pulse Width Modulation (PWM) signals to the active rectifier.

2.1. Wind Turbine

The turbine considered in this paper is a Horizontal Axis Wind Turbine (HAWT) with 3 blades whose length is R in (m) and which are fixed on a drive shaft rotating at the speed Ω_{turbine} in (rad·s^{-1}). Considering V_w the wind speed in (m·s^{-1}), ρ the air density in (kg·m^{-3}) (approximately 1.22 at atmospheric pressure), and the area opposed to the wind A in (m^2), the kinetic power of wind is expressed as follows:

$$P_w = \frac{\rho A V_w^3}{2}. \tag{1}$$

Then the power at the output of the turbine has this expression:

$$P_t = C_p(\lambda) P_w. \tag{2}$$

The power coefficient C_p is a function of the relative speed $\lambda = \dfrac{R\Omega_{\text{turbine}}}{V_w}$. This coefficient depends on the type of the turbine since it depends on the surface swept by the rotor whose size is different for different types of turbine.

2.2. Permanent Magnet Synchronous Generator

The PMSG model [9] is represented in the Park referential related to the rotating field, voltages expressions are:

$$v_d = -R_s i_d + L_q \omega_e i_q - L_d \frac{\mathrm{d}i_d}{\mathrm{d}t}, \tag{3}$$

$$v_q = -R_s i_q - L_d \omega_e i_d - L_q \frac{\mathrm{d}i_q}{\mathrm{d}t} + \sqrt{\frac{3}{2}} \Phi_{sf} \omega_e, \tag{4}$$

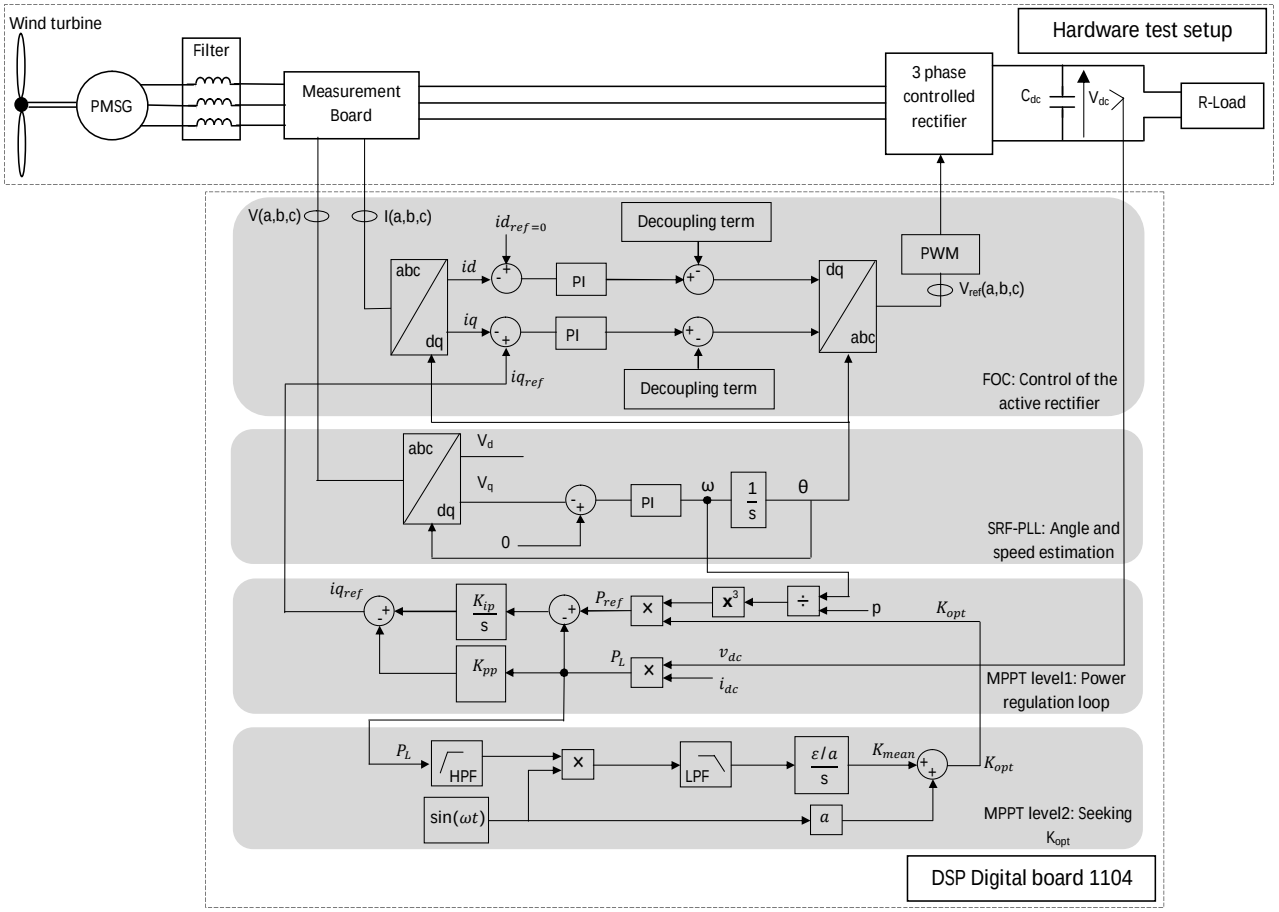

Fig. 1: Global structure.

where R_s is the stator resistance, L_d and L_q are the dq inductances, Φ_{sf} is the magnetic flux density, $\omega_e = p\Omega_{\text{turbine}}$ is the angular frequency and p is the number of pole pairs. Production of the electrical energy at the output of the generator causes a braking torque which has this expression:

$$T_e = -p\left(\sqrt{\frac{3}{2}}\Phi_{sf} i_q + (L_q - L_d) i_d i_q\right). \tag{5}$$

The mechanical equation is:

$$J\frac{\mathrm{d}\Omega_{\text{turbine}}}{\mathrm{d}t} = T_t + T_e - f\Omega_{\text{turbine}}, \tag{6}$$

where J is the total inertia, f is the viscous friction coefficient and $T_t = P_t/\Omega_{\text{turbine}}$ is the turbine torque.

2.3. FOC for the Active Rectifier

1) Study of Power Maximization

This study is realised to explain the motivation to use the FOC for the rectifier. The aim is to maximize the generator output power whose expression is:

$$P_g = v_a i_a + v_b i_b + v_c i_c = v_d i_d + v_q i_q. \tag{7}$$

Replacing elements of this equation by their expressions in Eq. (3) and Eq. (4) and considering the steady state characterized by no variations of currents and speed $\left(\frac{\mathrm{d}i_d}{\mathrm{d}t} = \frac{\mathrm{d}i_q}{\mathrm{d}t} = \frac{\mathrm{d}\Omega_m}{\mathrm{d}t} = 0\right)$ we deduce the following equations of P_g and the constraint of its maximization:

$$P_g = C_p\left(\frac{R\Omega_m}{V_w}\right) P_w - R_s\left(i_d^2 + i_q^2\right) - f\Omega_m^2, \tag{8}$$

$$\begin{aligned} C_p\left(\frac{R\Omega_m}{V_w}\right) P_w - f\Omega_m^2 = -T_e\Omega_m = \\ = \sqrt{\frac{3}{2}} p\Phi_{sf}\Omega_m i_q. \end{aligned} \tag{9}$$

A popular method allowing to realise this is the Lagrange multipliers whose first step is to define the Lagrange function as:

$$\begin{aligned} \zeta = P_g + \lambda_\zeta \cdot \ldots \cdot \\ \cdot \left(C_p\left(\frac{R\Omega_m}{V_w}\right) P_w - f\Omega_m^2 - \sqrt{\frac{3}{2}} p\Phi_{sf}\Omega_m i_q\right). \end{aligned} \tag{10}$$

The second step is to find a stationary point of this function by finding solution of the partial derivatives of

this function with respect to its four variables, results of this are given as follows:

$$\frac{\partial \zeta}{\partial i_d} = 0 \Rightarrow i_d = 0. \tag{11}$$

$$\frac{\partial \zeta}{\partial \lambda_\zeta} = 0 \Rightarrow i_q = \frac{C_p\left(\frac{R\Omega_m}{V_w}\right) P_w - f\Omega_m^2}{\sqrt{\frac{3}{2}} p \Phi_{sf} \Omega_m}. \tag{12}$$

$$\frac{\partial \zeta}{\partial i_q} = 0 \Rightarrow \lambda_\zeta = \frac{4R_s}{3p^2\Phi_{sf}^2}\left(f - \frac{P_w}{\Omega_m^2} C_p\left(\frac{R\Omega_m}{V_w}\right)\right). \tag{13}$$

$$\frac{\partial \zeta}{\partial \Omega_m} = 0 \Rightarrow \frac{R\Omega_m}{V_w}\frac{\mathrm{d}C_p\left(\frac{R\Omega_m}{V_w}\right)}{\mathrm{d}\lambda} = = \frac{\lambda_\zeta C_p\left(\frac{R\Omega_m}{V_w}\right) + (\lambda_\zeta + 2) f\Omega_m^2/P_w}{\lambda_\zeta + 1}. \tag{14}$$

From the first derivative Eq. (11) we deduce that P_g is maximised when $i_d = 0$, for that reason the FOC is selected as control of the implemented rectifier.

2) FOC Structure

The structure of the FOC [10] can be found in the Fig. 1 consisting of two current regulation loops based on the two similar transfer functions whose form is:

$$G(s) = \frac{i}{v} = \frac{-1}{R + Ls}. \tag{15}$$

Then

$$i = \frac{-1}{R + Ls}\left(K_{pc} i - \frac{K_{ic}}{s}\left(i_{ref} - i\right)\right), \tag{16}$$

$$\frac{i}{i_{ref}} = \frac{\frac{K_{ic}}{L}}{s^2 + \frac{R + k_{pc}}{L} s + \frac{K_{ic}}{L}}. \tag{17}$$

Finally, we extract a second order equation with the following form:

$$\frac{i}{i_{ref}} = \frac{\omega_n^2}{s^2 + 2\xi\omega_n s + \omega_n^2}. \tag{18}$$

We consider the same parameters for both currents i_d and i_q, then coefficients $K_{ic} = L\omega_n^2$ and $K_{pc} = 2\xi\omega_n L - R$ are the same for the two control loops. As illustrated, Park and inverse Park transformations in this control require the angle θ estimated by the SRF-PLL. From v_d and v_q expressions, we deduce that a decoupling of the two currents control loops is necessary. Then the decoupling terms are:

$$DT_d = \omega_e L_q i_q, \tag{19}$$

$$DT_q = -\omega_e L_d i_d + \omega_e \sqrt{\frac{3}{2}} \Phi_{sf}. \tag{20}$$

3. Sensorless MPPT

As outlined in the introduction, the aim of this work is to build a complete MPPT strategy for the proposed WECS detailed in Fig. 1 from which we can observe that the MPPT algorithm has two levels the first is a power regulation loop generating at its output the i_{qref} for the FOC and the second is an extremum seeking system giving the value of the K_{opt}. Generator rotor speed needed is estimated using the SRF-PLL.

3.1. SRF-PLL as Angle and Speed Estimator

The SRF-PLL [11] is based on aligning the output frequency with the d axis in the dq frame by using a PI controller to force the q component voltage to zero. Referring to Fig. 1 which shows the basic structure of the SRF-PLL, the voltages in dq frame V_d and V_q are deduced from the three phase voltages V_a, V_b and V_c using Park's transform including the estimated phase angle θ:

$$\begin{bmatrix} V_d \\ V_q \\ V_0 \end{bmatrix} = \frac{2}{3}\begin{bmatrix} \sin(\theta) & \sin(\theta - \frac{2\pi}{3}) & \sin(\theta - \frac{4\pi}{3}) \\ \cos(\theta) & \cos(\theta - \frac{2\pi}{3}) & \cos(\theta - \frac{4\pi}{3}) \\ \frac{1}{2} & \frac{1}{2} & \frac{1}{2} \end{bmatrix}\begin{bmatrix} V_a \\ V_b \\ V_c \end{bmatrix}. \tag{21}$$

To align the SRF-PLL output with d axis, the PI controller forces the component to zero. When this output becomes in-phase with the supply voltage, the PI output will be equal to ω. Then the angle θ can be obtained by integrating the PI output as shown.

3.2. MPPT Level 1: Power Regulation Loop

We consider the expression of the turbine generated power to extract the area where the points of maximum power are located. That is the curve described using the following expression:

$$P_{opt} = \frac{1}{2}\rho A\left(\frac{R\Omega_m}{\lambda_{opt}}\right)^3 C_{popt} = K_{opt}\Omega_m^3, \quad \text{with } K_{opt} = \frac{\rho A R^3 C_{popt}}{2\lambda_{opt}^3}. \tag{22}$$

As we have shown, the MPPT principle must be applied to the entire conversion chain. Then we constructed a power control loop based on the knowledge of the optimum power value, the reference power is obtained from the estimated rotational speed and the value of the K_{opt} parameter. The structure of this loop is illustrated in Fig. 1.

3.3. MPPT Level 2: Seeking K_{opt}

For our case, we suppose that characteristics of the wind turbine are undefined, so the value of K_{opt} is undetermined. To determine this value continuously an automatic system is implemented, this system is a method of extremum seeking [12] presenting a second level of the MPPT. This block, as Fig. 1 describes, determines an average value K_{mean} and adds a very slow sinusoidal perturbation to this value to generate the value of K_{opt} used as an input for the power control loop. Finally, we obtain variations in the average value of instantaneous power P_{inst} according to variations of the K_{opt} value at the output of a high pass filter. The low pass filter rejects the frequency of the disturbance signal at the output of the multiplier. Gain a is the disturbance signal amplitude and ε adjusts the integrator gain which defines K_{mean} value.

4. Experimental Results

The proposed control system was implemented using real time digital controller dSPACE 1104. This controller and the hardware test setup consisting of a 5 kW PMSG, wind turbine emulator, three phase rectifier and a DC load $R = 115.1\ \Omega$ are presented in Fig. 2.

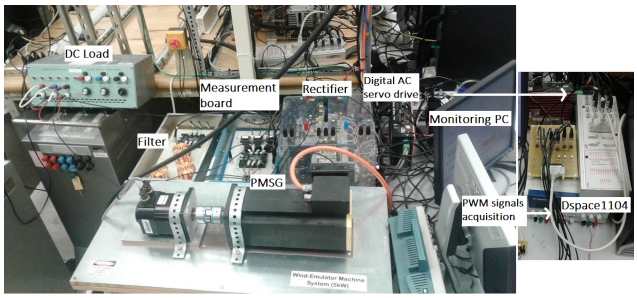

Fig. 2: Experimental test bed setup.

This paper considers a variable speed wind conversion system for investigation. To evaluate its performance and as illustrated in Fig. 3, a variable wind speed profile in the form of a repeating sequence of different values of the wind speed is considered.

According to Fig. 4, where the estimated position by the SRF-PLL and one of the three phase voltages precisely V_a are presented, the SRF-PLL is operating accurately, and this is clearer in the zoom.

The second estimated parameter by the SRF-PLL needed in the system control of our sensorless MPPT structure is the generator speed which is presented with the real generator speed in Fig. 5. It appears that values of the two speeds are close and also vary simultaneously.

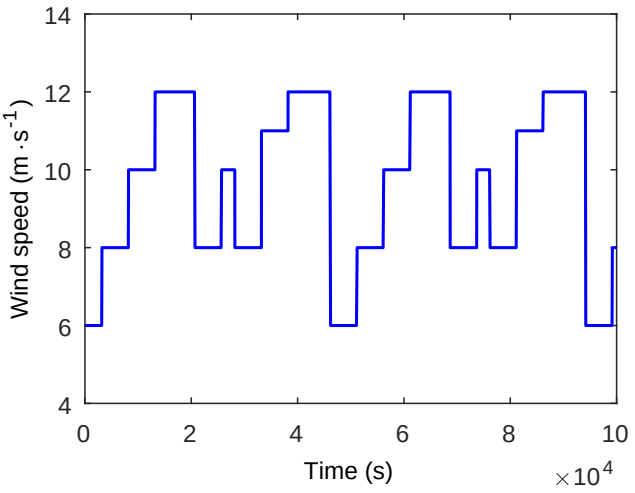

Fig. 3: Variable wind speed profile.

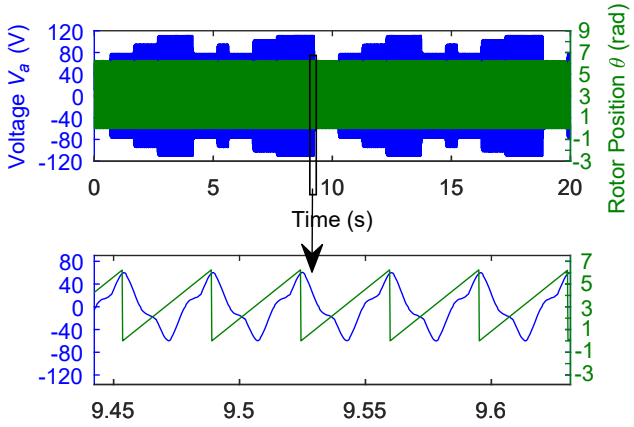

Fig. 4: Voltage V_a (V) and the enstimated Rotor position (rad).

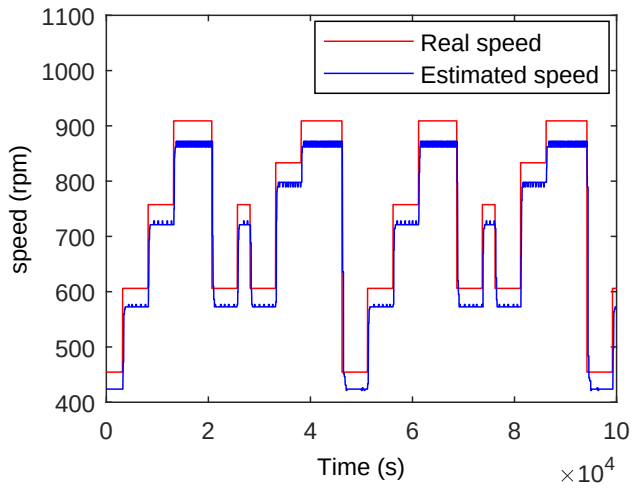

Fig. 5: Real generator speed (rpm) and estimated generator speed (rpm).

Figure 6 shows the generator output three phase voltages. To better visualise variations of this three phase voltages, a zoom in on a smaller section of the time line was applied.

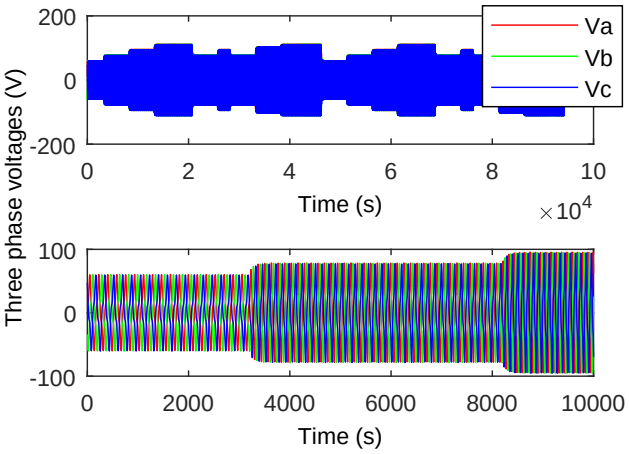

Fig. 6: Generator output three phase voltages.

The DC voltage and current are presented in Fig. 7 varying with the variable wind speed profile. Values of this two outputs are in accordance with the measurements carried out in real time during the experiments.

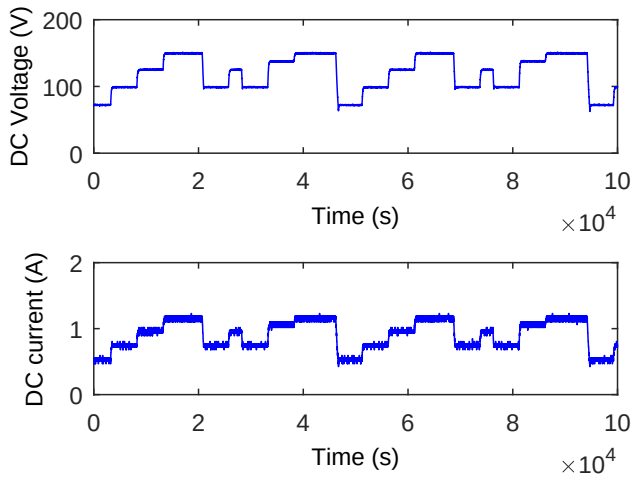

Fig. 7: DC voltage (V) and DC current (A).

Finally, Fig. 8 presents variations of both the DC power at the resistive load and the active generator output power.

5. Conclusion

In this paper, a sensorless two-level MPPT strategy was applied to a variable speed wind energy conversion system composed of a wind turbine, a PMSG and an active rectifier connected to a DC load. The complete structure is presented in Fig. 1.

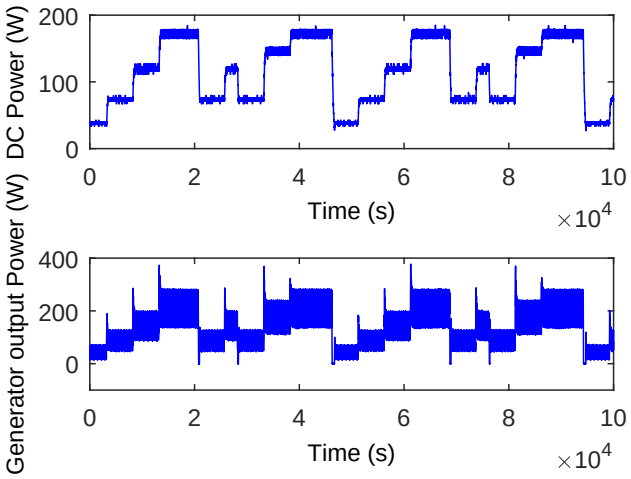

Fig. 8: Power at the DC load (W) and Power at the generator output (W).

An analysis of the generator power maximization was discussed previously justifying the use of the FOC generating the PWM signals to the active rectifier.

The approach that has been used in this work aims to avoid the mechanical sensors for their aforementioned disadvantages, for this reason, an SRF-PLL was employed as a speed and angle estimator which are inputs of the FOC and the MPPT blocks.

The MPPT strategy adopted has two levels; the first level is a power regulation loop generating the value of i_{qref} needed in the FOC and taking as input the value of K_{opt} the coefficient that includes the turbine parameters and estimated by the second level which is a method of the extremum seeking.

An experimental setup with a 5 kW PMSG including a real time digital controller dSPACE 1104 was designed in order to validate the described approach.

From the last section where the experimental results are analysed and shown, it is apparent that the estimated speed by the SRF-PLL follows the real generator speed and then the main aim of employing the SRF-PLL is reached. Also from figures illustrating the power at the DC load and power at the generator output, we can deduce that the MPPT strategy adopted gives optimal extracted power from the studied WECS. As can be seen from the other obtained results, the whole introduced strategy is achievable in real time applications and can be replaced by other MPPT algorithms according to the needs and objectives of the system control.

Future work will investigate the comparison between the different estimators used in our previous works as outlined in the introduction, and the estimator employed in this work.

Acknowledgment

The authors gratefully acknowledge the support of the Energy Systems Research Laboratory, Department of Electrical and Computer Engineering, in Florida International University, Miami, FL 33174 USA, in which the experimental test setup was built and the experimental results were validated.

References

[1] MARUF HOSSAIN, M. and H. ALI. Future research directions for the wind turbine generator system. *Renewable and Sustainable energy reviews*. 2015, vol. 49, iss. 1, pp. 481–489. ISSN 1364-0321. DOI: 10.1016/j.rser.2015.04.126.

[2] LI, S., T. A. HASKEW, R. P. SWATLOSKI and W. GATHINGS. Design, Optimal and direct-current vector control of direct-driven PMSG wind turbines. *IEEE Transactions on Power Electronics*. 2012, vol. 27, iss. 5, pp. 2325–2337. ISSN 0885-8993. DOI: 10.1109/TPEL.2011.2174254.

[3] POLINDER, H., F. F. A. VAN DER PIJL, G. J. DE VILDER and P. J. TAVNER. Comparison of direct-drive and geared generator concepts for wind turbines. *IEEE Transactions on Energy Conversion*. 2006, vol. 21, iss. 3, pp. 725–733. ISSN 0885-8969. DOI: 10.1109/TEC.2006.875476.

[4] MERZOUG, M. S. and F. NACERI. Comparison of Field-Oriented Control and Direct Torque Control for Permanent Magnet Synchronous Motor (PMSM). *International Journal of Electrical, Computer, Energetic, Electronic and Communication Engineering*. 2008, vol. 2, no. 9, pp. 1797–1802. ISSN 5372-7291.

[5] KALA, H. and K. S. SANDHU. Effect of change in power coefficient on the performance of wind turbines with different dimensions. In: *International Conference on Microelectronics, Computing and Communications*. Durgapur: IEEE, 2016, pp. 1–4. ISBN 978-1-4673-6622-9. DOI: 10.1109/MicroCom.2016.7522487.

[6] ECHCHAACHOUAI, A., S. EL HANI, A. HAMMOUCH and S. GUEDIRA. A new Sensorless Maximum Power Point Tracking Technologies od Wind Conversion Chain based on a PMSG. In: *International Renewable and Sustainable Energy Conference*. Ouarzazate: IEEE, 2014, pp. 1–6. ISBN 978-1-4799-7337-8. DOI: 10.1109/IRSEC.2014.7059789.

[7] ECHCHAACHOUAI, A., S. EL HANI, A. HAMMOUCH and S. GUEDIRA. Extended Kalman Filter used to estimate speed rotation for sensorless MPPT of wind conversion chain based on a PMSG. In: *International Conference on Electrical and Information Technologies*. Marrakech: IEEE, 2015, pp. 172–177. ISBN 978-1-4799-7479-5. DOI: 10.1109/EITech.2015.7162989.

[8] TAN, Y., W. MOASE, C. MANZIE, D. NESIC and I. MAREELS. Extremum seeking from 1922 to 2010. In: *Proceedings of the 29th Chinese Control Conference*. Beijing: IEEE, 2010, pp. 14–26. ISBN 978-1-4244-6263-6.

[9] BHENDE, C. N., S. MISHRA and S. G. MALLA. Permanent Magnet Synchronous Generator-Based Standalone Wind Energy Supply System. *IEEE Tansactions on Sustainable Energy*. 2011, vol. 2, iss. 4, pp. 361–373. ISSN 1949-3029. DOI: 10.1109/TSTE.2011.2159253.

[10] KIRAN, Y. and P. S. PUTTASWAMY. Field Oriented Control of a Permanent Magnet Synchronous Motor using a DSP. *International Journal of Advanced Research in Electrical, Electronics and Instrumentation Engineering*. 2014, vol. 3, iss. 10, pp. 12364–12378. ISSN 2320-3765.

[11] YOUNG, K. and R. A. DOUGAL. SRF-PLL with dynamic center frequency for improved phase detection. In: *International Conference on Clean Electrical Power*. Capri: IEEE, 2009, pp. 212–216. ISBN 978-1-4244-2543-3. DOI: 10.1109/ICCEP.2009.5212055.

[12] AUBREE, R., F. AUGER and R. DAI. A new low-cost sensorless MPPT algorithm for small wind turbines. In: *First International Conference on Renewable Energies and Vehicular Technology*. Hammamet: IEEE, 2012, pp. 305–311. ISBN 978-1-4673-1168-7. DOI: 10.1109/REVET.2012.6195288.

About Authors

Amina ECHCHAACHOUAI was born in Morocco in 1990. She received the university degree in Electrical Engineering before being an engineer Networks and Telecommunications from the National School of Applied Sciences, Fes, Morocco. She is currently working towards the Ph.D. degree at The Department of Electrical Engineering in the Mohammed V Souissi University, ENSET-Rabat and her main research interest is in the control of a wind conversion chain based on a PMSG.

Soumia EL HANI Professor of Electrical Machine and drives at the Ecole Normale Superieure de

Enseignement Technique (ENSET), Mohammed V University Rabat, Morocco since 1992. She obtained her engineering degree From Higher school of Mines-Rabat, and her Ph.D. in Automatic from Mohammedia School of Engineering, Rabat Morocco in 2003. Her research interests are in the area of Robust Control, Monitoring and Diagnosis of Electromechanical Systems. She in charge of the research team 'Energy Optimisation, Diagnosis and Control' EODIC, research Laboratory in Energy, Electrotechnic, Robotic and Automatic. She is Author of several publications in the field of electrical engineering, including robust control systems, diagnosis and control systems of wind electric conversion. She has supervised Ph.D. and Masters Theses dealing with different research topics concerned with her research interests. Soumia El Hani is Prof. Dr. IEEE senior member, she was a member of the Organizing and the Scientific Committees of several international conferences dealing with topics related to Renewable Energy, Electrical Machines and Drives. Since the year 2015, Soumia El Hani is the co-founder and general co- chair of 'The International Conference on Electrical and Information Technologies'. Also, she is the co-editor of ICEIT 2015 and ICEIT 2016 Proceedings.

Ahmed HAMMOUCH received the master degree and the Ph.D. in Automatic, Electrical, Electronic by the Haute Alsace University of Mulhouse (France) in 1993 and the Ph.D. in Signal and Image Processing by the Mohammed V University of Rabat in 2004. From 1993 to 2013 he was a professor in the Mohammed V University in Morocco. Since 2009 he manages the Research Laboratory in Electronic Engineering. He is an author of several papers in international journals and conferences. His domains of interest include multimedia data processing and telecommunications. He is with National Center for Scientific and Technical Research in Rabat.

Imad ABOUDRAR was born in Agadir, Morocco. He received the M.Sc. degree in electrical engineering in 2016 from the Mohammed V University, Rabat Morocco- where he is currently working toward the Ph.D. degree in the department of electrical engineering. Since 2016, His research interests are related to renewable energy, His current activities include the improvement of energy quality of an integrated PV and Wind Hybrid System connected to the grid.

Appendix A Experimentation PMSG Parameters

- Output power = 0–5 kW,
- Rated voltage = 208 Vrms,
- Rated speed = 1200 rpm,
- Resistance = 0.46 Ω,
- Inductance = 4.86 mH.